

On the Electrical Properties of LiNO_3

J. H. FERMOR and A. KJEKSHUS

Kjemisk Institutt A, Universitetet i Oslo, Blindern, Oslo 3, Norway

The electrical resistivity and dielectric constant of anhydrous, polycrystalline samples of LiNO_3 have been measured over the temperature range from -70 to 210°C , and the resistivity of zone refined samples determined from 80°C to the melting point. The results indicate the occurrence of a solid state transition at -10°C , and exhibit a further anomaly at 230°C . The data are discussed in relation to those for NaNO_3 .

Lithium nitrate crystallizes with the calcite type structure¹ which is reported^{2,3} as being retained between room temperature and the melting point (251.4°C ⁴). The only solid state transition recorded in the literature is one of an unspecified nature which was deduced from ultra-violet absorption data as occurring at 170°C .⁵ Very little information is available on other properties of LiNO_3 ,^{6,7} and in particular, no electrical data have been published hitherto.

The present measurements were performed as part of an investigation of the transformations and order-disorder properties of anhydrous nitrates.⁸⁻¹¹

EXPERIMENTAL

Lithium nitrate is deliquescent, and rapidly absorbs water from the atmosphere. Small crystals were, however, found to be easily dried by heating to $\sim 120^\circ\text{C}$ under vacuum for a few hours. In preparing samples for the measurement of dielectric properties above and below room temperature, LiNO_3 crystals (Riedel de Haën AG) were dried in this way, before melting between 1.0 mm thick electrode plates of silver, having an area of 9.0 cm^2 , at a spacing of $\sim 0.3\text{ mm}$. Larger samples were also formed in the same way between 5.0 mm thick silver plated electrodes, for additional measurements above room temperature.

Measurements were obtained on cooling samples to room temperature from the melting point within a sample holder¹⁰ containing P_2O_5 as a desiccating agent, while the samples to be measured below room temperature were cooled more rapidly (over $\sim 30\text{ min}$) in the dry environment, and sealed at $\sim 50^\circ\text{C}$ with varnish to prevent the ingress of moisture. The latter samples were then transferred to the dry nitrogen environment of the low temperature sample holder⁹ without delay, and measurements were commenced immediately.

Measurements on zone refined samples were obtained using a cylindrical quartz sample holder equipped with silver electrodes, which was situated in the zone melting apparatus⁸ during the course of the experiment. Approximately 15 passes of the molten zone were made at a speed of 10 cm/h before measurements were commenced. Sample

temperatures were measured in this case by means of a Chromel-Alumel thermocouple used in conjunction with a digital voltmeter (Dynamco Instruments Ltd., DM 2006).

All values of sample capacitance, dissipation, and a.c. (1 kHz) and d.c. resistance, were obtained with the aid of an impedance bridge (General Radio, 1650-A).

In order to achieve thermal equilibrium, ~ 30 min were allowed to elapse between successive measurements, which provided stable readings for all samples.

Analyses of the impurity contents of the investigated samples were obtained using the methods of atomic absorption and mass spectrometry. The application of the latter method was somewhat hindered by the formation of hydrocarbons resulting from reactions between water absorbed by the salt and the graphite electrode. The analyses yielded impurity contents (in ppm) for the untreated and zone refined samples as follows, the latter quantities being shown in parenthesis: Na 830 (340), K 170 (170), Rb ~ 10 (~ 5), Cs ~ 10 (~ 5), Be 0.1 (~ 0), Mg 0.1 (0.01), Ca 240 (35), Sr 10 (~ 1), and Ba ~ 10 (~ 5). (Transition metals as impurities were present in amounts < 1 ppm in all samples.) Of the substantial impurity contents, zone refinement notably reduced those of sodium and calcium by factors of 2.5 and 7, respectively, whereas that for potassium remained unchanged.

RESULTS

Values of the dielectric constant ϵ for polycrystalline LiNO_3 , over the temperature range from -70 to 30°C are presented in Fig. 1, for conditions of both decreasing and increasing temperature. Measurements on two further samples showed the results to be reproducible.

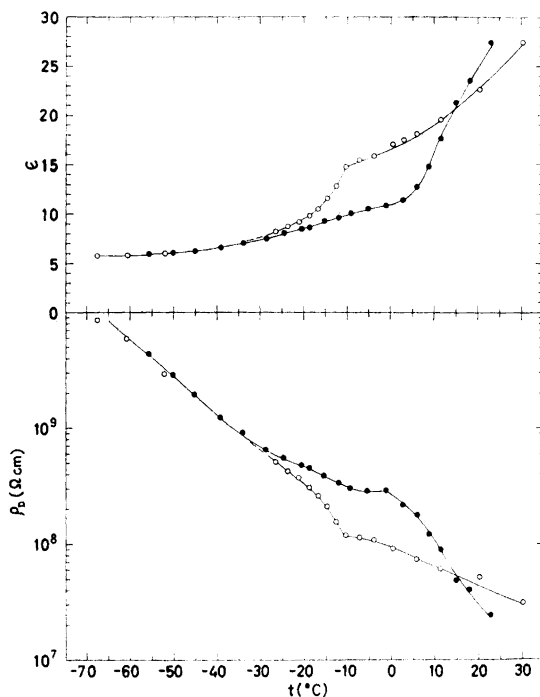


Fig. 1. Dielectric constant ϵ and resistivity ρ_D as functions of temperature for polycrystalline LiNO_3 . Open circles denote measurements with decreasing temperature, filled circles with increasing temperature.

On decreasing the temperature from 30°C , ϵ falls regularly with a decreasing slope, to -10°C , where a discontinuous increase in the value of the slope is observed. On further decrease of temperature, ϵ approaches a value of 5.8 asymptotically at -70°C .

The ϵ -curve obtained on increasing the temperature departs from that described above at $\sim -25^\circ\text{C}$ to form a loop which closes at 15°C , where the two curves cross.

Corresponding values of the resistivity ρ_D^* are also plotted in Fig. 1, the curves showing a close correlation with the temperature dependence of ϵ , in that a discontinuity of slope occurs at -10°C , and a loop is formed between the curves for decreasing and increasing temperature.

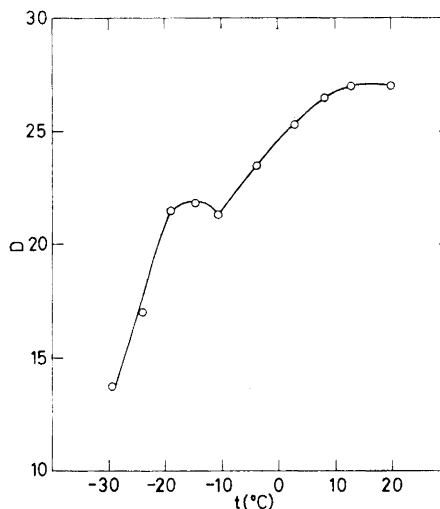


Fig. 2. Dissipation D as a function of decreasing temperature for polycrystalline LiNO_3 .

Measured values of D ($=1/\omega R_p C_p$, where R_p is the equivalent parallel resistance of the sample), for another sample over the anomalous region, are given in Fig. 2. D is a function of both ϵ and ρ_D , and being independent of the dimensions of the sample, is a convenient parameter for study in relation to anomalies of this kind. The curve comprises two branches forming a cusp at -10°C , thus confirming the temperature of the anomaly on cooling.

The values of ϵ and ρ_D obtained above room temperature (confirmed by measurements on two other samples) are shown in Fig. 3. In the region between the melt and 210°C , the dissipation was greater than the maximum value measurable ($D_{\text{max}}=50$). Below 210°C , ϵ and ρ_D vary non-linearly with temperature, the magnitudes of the slopes of the curves increasing with increasing temperature.

* $\rho_D = S/(\omega C_p D t)$, where ω is the angular frequency, C_p the equivalent parallel capacitance of the sample, D the dissipation, t the sample thickness, and S the electrode area.

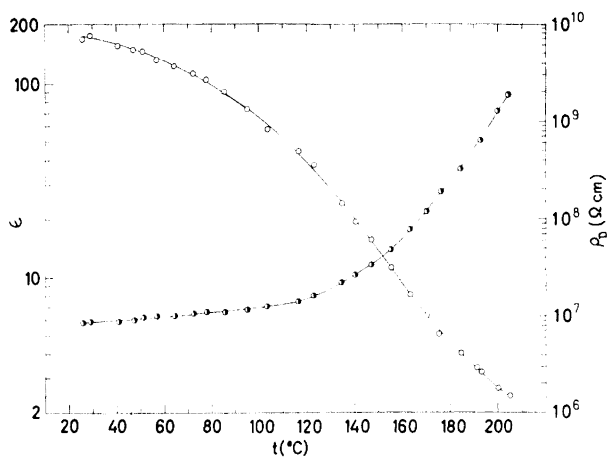


Fig. 3. Dielectric constant ϵ (half filled circles) and resistivity ρ_D (open circles) as functions of decreasing temperature for polycrystalline LiNO_3 .

At temperatures down to $\sim 120^\circ\text{C}$ values of a.c. resistance could also be accurately determined, and the values of ρ_{AC} coincide precisely with those of ρ_D in Fig. 3. At lower temperatures, the a.c. sample resistance exceeded that which could be measured with satisfactory accuracy using the present method.

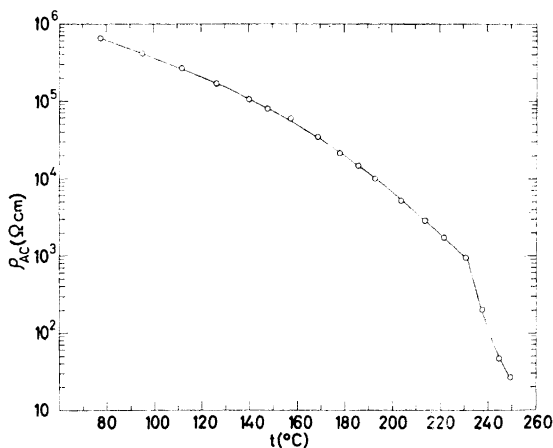


Fig. 4. Resistivity ρ_{AC} at 1 kHz for zone refined LiNO_3 as a function of decreasing temperature.

The a.c. resistivity at 1 kHz for a zone refined sample comprising a number of single crystals, is plotted in Fig. 4, from 80°C to close to the melting point. The curve, which extends over 4.5 decades of resistivity value, is composed

of two well defined sections, connected with a discontinuity of slope at 230°C . The temperature coefficient of resistivity is negative over the whole region, and numerically greater at the higher temperatures. Accurate measurements of d.c. resistivity of this sample were also possible at temperatures above $\sim 140^\circ\text{C}$, yielding values which are some 10 % higher than those for ρ_{AC} , due to polarization.

DISCUSSION

Great care was taken in the present experiments to prevent contamination of the samples by water, but complete exclusion is unlikely and some reserve may be indicated in interpreting the results. However, the difference in thermal histories between the low and high temperature samples appears to be responsible for the discrepancies in the electrical parameters at room temperature, which are found in Figs. 1 and 3. The differences are consistent with a greater degree of lattice disorder in the rapidly cooled samples.

The anomaly at -10°C in the cooling curve for ϵ in Fig. 1 is very similar in form to that found at -30°C in the case of NaNO_3 .¹⁰ The ρ_D versus t relationship (Fig. 1) also resembles the corresponding data for NaNO_3 . The two anomalies are thus clearly of the same kind, and as in the case of NaNO_3 , that in LiNO_3 is attributed to the effects of a structural transition. The changes in ϵ and ρ_D across the anomaly, are consistent with the low temperature phase having a more rigid lattice, where the ions are situated in narrower and deeper potential wells (inferred from the steeper ρ_D -curve below -10°C in Fig. 1).

The values of ϵ and ρ_D obtained above room temperature (Fig. 3) are also similar to the corresponding variations in these parameters for NaNO_3 .¹⁰ Since LiNO_3 and NaNO_3 are isostructural at room temperature, the close resemblance of the electrical characteristics implies that the temperature dependence of the periodic potential is very similar for the two lattices. In the case of NaNO_3 , a second order transformation between 160 and 275°C , involving rotational disorder of the nitrate group, has been well established by means of X-ray diffraction and heat capacity measurements, and this information provided a basis of interpretation of the electrical data. No useful calorimetric data¹² are available for LiNO_3 , however, and X-ray studies^{2,3} at high temperatures have been concerned with the symmetry of the unit cell rather than possible disorder of the nitrate group. Nevertheless, it is suggested by analogy, that the results shown in Figs. 3 and 4 reflect the occurrence of a transition over the temperature range 120 to 230°C , whose nature is similar to that in NaNO_3 . It is of interest to note that the earlier mentioned transformation temperature of 170°C ⁵ falls in the middle of this range.

The application of an alternating electric field to an ionic solid, produces, on the average, a displacement of some charges through the lattice, thus creating a resistive component of the sample current in phase with the applied field. In addition, there are charges which remain localized, but oscillate with a phase angle which at low frequencies differs by $\pm\pi/2$ from that of the applied field. The oscillatory motion provides a capacitive component of the sample current. The measured increase of more than tenfold in ϵ over the temperature interval 120 to 200°C (Fig. 3) thus implies a virtual collapse of the potential barriers containing the ions.

In order to investigate in detail that portion of the a.c. resistivity curve of Fig. 4 which lies close to the melting point, a part of the results have also been plotted as a function of the reciprocal of the absolute temperature in Fig. 5. Neglecting the unusual curvature close to the melting point, the curve

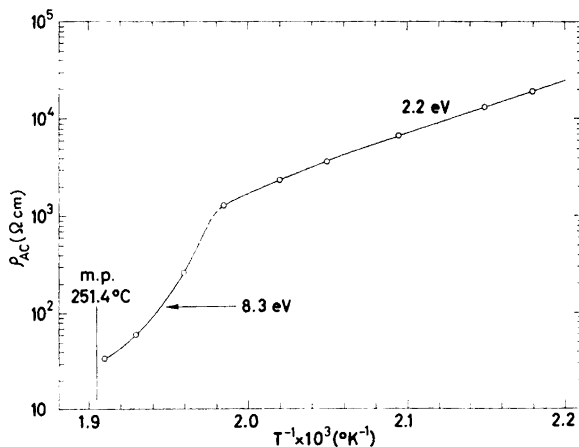


Fig. 5. Resistivity ρ_{AC} (1 kHz) for zone refined LiNO_3 versus reciprocal absolute temperature.

may be discussed in two parts. Below 230°C , the curve is characterized by the well defined energy gap $W=2.2$ eV, calculated according to the conventional expression for ionic resistivity $\rho=\rho_0\exp(W/2kT)$, while the mean apparent value at higher temperatures is 8.3 eV. As with NaNO_3 , where the corresponding figure is 9.1 eV, it seems unlikely that such a high value is characteristic of a normal mechanism of ion transport, which would require interpretation in terms of a transition either between two dominant intrinsic mechanisms (interstitial-vacancy, cation-anion, cation-electron, etc.) or between an extrinsic and an intrinsic type of conduction. The implied rotational disorder of the nitrate group above 230°C is more compatible with a decrease than an increase in energy barriers and one concludes, therefore, that the steep fall of resistivity with increasing temperature close to the melting point is due to an anomalous increase in the number and mobility of activated cations, leading to temperature dependent energy parameters in the region. This phenomenon, which is clearly an important precursor of melting, is a direct consequence of the reduction of energy barriers as the degree of disorder increases on approaching the melting point.

The zone refined sample has a resistivity ρ_{AC} which is some three orders of magnitude lower than ρ_D for the starting material, while the temperature coefficients of resistivity are very similar. The effect of refinement on resistivity is in the opposite sense to that which would result from the removal of an impurity responsible for the creation of extrinsic charge carriers, by reason of a low activation energy, or by the introduction of lattice vacancies according

to the Wagner effect. The independence of energy parameter on purity also supports the hypothesis that conduction is intrinsic and predominantly by the small Li^+ ions ($r \approx 0.6 \text{ \AA}$) in both specimens. The observed increase in conductivity on zone refinement is thus due to the improved microscopic and macroscopic order produced in the sample, and a consequent reduction in scattering and trapping of the carriers by impurities.

Acknowledgements. This work was made possible by the kind provision of laboratory facilities by Professor H. Haraldsen, and the financial support of *Norges almenvitenskapelige forskningsråd*.

REFERENCES

1. Zachariasen, W. H. *Skrifter Norske Vidensk. Akad. Oslo* **1928**, No. 4.
2. Kracek, F. C., Barth, T. F. W. and Ksanda, C. J. *Phys. Rev.* **40** (1932) 1034.
3. Fischmeister, H. F. *J. Inorg. Nucl. Chem.* **3** (1956) 182.
4. Lehrman, A. and Breslow, D. *J. Am. Chem. Soc.* **60** (1938) 873.
5. Rhodes, E. and Ubbelohde, A. R. *Proc. Roy. Soc. (London)* **A 251** (1959) 156.
6. McLaren, A. C. *Rev. Pure Appl. Chem.* **12** (1962) 54.
7. Ferraro, J. R. and Walker, A. *J. Chem. Phys.* **42** (1965) 1273.
8. Fermor, J. H. and Kjekshus, A. *Acta Chem. Scand.* **21** (1967) 1265.
9. Fermor, J. H. and Kjekshus, A. *Acta Chem. Scand.* **22** (1968) 836.
10. Fermor, J. H. and Kjekshus, A. *Acta Chem. Scand.* **22** (1968) 1628.
11. Fermor, J. H. and Kjekshus, A. *Acta Chem. Scand.* **22** (1968) 2054.
12. Goodwin, H. M. and Kalmus, H. T. *Phys. Rev.* **28** (1909) 1.

Received October 5, 1968.